Characterization of the activity of Roco4 and identifying its substrates

Lianne Fikse, M.Sc.

Supervisors: K.E.Rosenbusch and A. Kortholt

Department of Cell Biochemistry, University of Groningen, the Netherlands

October 2016

Point mutations of Leucine Rich Repeat Kinase 2 (LRRK2) are known to be pathogenic and lead to Parkinson's disease (PD). Recent studies have shown specific Rab proteins are a substrate of LRRK2 and, through their interaction with LRRK2, influence processes such as endosomal budding. However, as LRRK2 has proven to be difficult to isolate, the homologous Roco4 from *Dictyostelium discoideum* is used. This study aims to determine whether various Rab proteins are substrates of Roco4 *in vitro*, and whether they exhibit any protein-protein interaction. Radioactive kinase assays are used to understand which Rabs are substrates. Possible substrates are then studied through radioactive kinetics assays and pull-down assays. We found that Rab1D and possibly Rab8B are substrates for *Dictyostelium* Roco4, and therefore may contribute to the PD phenotype.

Parkinson's disease (PD) is a neurodegenerative disorder, characterized by tremors, dyskinesia, rigidity, and instability and mild cognitive impairment. It causes loss of dopaminergic neurons in the substantia nigra, and the formation of pathogenic protein aggregates called Lewy bodies in dopaminergic neurons. PD has been found to mainly affect the elderly; only 10% of the patients are younger than 45 years and incidence rises sharply with age (Lees AJ, et al. 2009). This indicates ageing might play a key role in developing PD. With 1 – 2% of the elderly population affected worldwide (Lees AJ, et al. 2009) it is a common disorder, and a curative treatment has not been found thus far. Causes of PD include genetic predisposition and environmental factors, but to what extent and in what way they influence the development of the disease is yet to be determined. There are two forms of PD; sporadic (often idiopathic) and familial. It is expected that the number of sporadic cases will decrease over the years, as research will reveal more pathogenic factors.

Genome-wide association studies have shown that mutations in certain genes (PARK2/7, PINK1, SNCA and LRRK2) increase the susceptibility to PD (Sanchez SJ, et al. 2009) (Nails MA, et al. 2011). Leucine Rich Repeat Kinase 2 (LRRK2) has been found to be affected in sporadic as well as familial PD. Seven common point mutations in LRRK2 have been found to be pathogenic: R1441C/G/H, I1122V, Y1699T, L1180T and G2019S. The most common pathogenic mutation associated with late-onset autosomal dominant PD is G2019S; 1% of sporadic PD patients and 4% of hereditary PD patients have this mutation (Healy DG, 2008).

The G2019S mutation is located in the kinase domain of LRRK2. Kinases phosphorylate their target proteins by transferring the ɣ-phosphate of an ATP molecule to the phosphorylation site in the target protein. This is a very common regulatory mechanism and is used in numerous signal transduction pathways. Multiple studies show that the G2019S mutation results in significantly enhanced kinase activity (Gómez-Suaga P, et al. 2014) (Ho FY, et al. 2014) (Jaleel ref 2007) (Khan NL, et al. 2005) (West AB, et al. 2005). These findings suggest that increased kinase activity could play a role in the development of PD. However, another mutation in the kinase domain, I2020T, does not affect kinase activity, but remarkably enough also results in PD activity (Gómez-Suaga P, et al. 2014) (Ho FY, et al. 2014) (Jaleel M, et al. 2007) (Khan NL, et al. 2005) (West AB, et al. 2005).

LRRK2 is a member of the Ras/GTPase family of Roco proteins, which are characterized by conserved Roc and COR domains (Marin I, et al. 2008). LRRK2 is a

large protein, consisting of the following domains: an armadillo repeats (ARM) domain, an ankyrin repeat (ANK) domain, a leucine-rich repeat (LRR) domain, a Ras-of-complex proteins/ G-domain (Roc) domain, a C-terminal of Roc (COR) domain, and a WD40 domain (Fig. 1). LRRK2 has many functions and is involved in multiple pathways, such as Wnt signalling, autophagy, regulation of neurite growth, mitochondrial (dys)function, and cytoskeletal dynamics (Dächsel JC, et al. 2010) (Esteves AR, 2016) (Winner B, et al. 2011).

Currently, scientific research on LRRK2 mainly focusses on the dysregulation of LRRK2 caused by the known mutations and their effects in relation to the cell. It has been reported that several processes are affected when the G2019S mutation is introduced in LRRK2, such as autophagy, mitochondrial functioning and vesicular trafficking (Su Y, Qi X. 2013). Recent studies have shown that proteins of the Rab family are a substrate of LRRK2 and, through interaction with LRRK2, influence processes such as vesicle endocytosis and endosomal budding (Gómez-Suaga P, et al. 2014) (Steger M, et al. 2016) (Yun HJ, et al. 2015) Rab proteins are GTPases and are often referred to as molecular switches. The Rab proteins have more interesting links to PD rather than just potential LRRK2 interaction. Enhanced expression levels of Rab1, Rab3A, and Rab8A have been proven to rescue the dopaminergic neuron loss caused by the toxic α-synuclein aggregates in animal models of PD (Cooper AA, et al. 2006) (Gitler AD, et al. 2008). All of these implications of Rabs and LRRK2 being involved with PD make these two proteins the focus of this study.

Since the 1980s, kinase inhibitors have been used as treatment for various diseases and disorders, and they also could potentially be an interesting drug for PD. LRRK2 (kinase) inhibitors could be used to treat PD patients with the G2019S mutation in the LRRK2 gene, so the enhanced kinase activity is decreased or, ideally, even normalized. Examples of LRRK2 inhibitors that have been recently discovered are staurosporine (Covy JP, Giasson BI. 2009), LRRK2-Inh-1 (Deng X. 2011), and MLi-2 (Fell MJ, et al. 2015). While they rescue the neurodegenerative phenotype in varying degrees, unfortunately, all of the aforementioned inhibitors have shown serious off-target effects when tested on animal models. Side effects include renal abnormalities and pulmonary toxicity. These critical safety concerns prevent LRRK2 inhibitors from being used in clinical trials.

It has been challenging to isolate LRRK2 and its separate domains in sufficient quality to use for research. Previous attempts have shown that LRRK2 cannot be expressed in *Escherichia coli*, and purified full-length LRRK2 can be unstable, bound to chaperones or missing certain essential interactors (Gilsbach BK, et al. 2012). Therefore, a homologous protein is often used for studies involving LRRK2. Whereas humans have four Roco proteins from the Roco family, DAPK1, MFHAS1, LRRK1, LRRK2, *Dictyostelium discoideum* has eleven Roco proteins. Roco4 bears the most homology to LRRK2, especially the kinase domain, which is why Roco4 is used in this study. The PD mutations of G2019S and I2020T and their effects on the kinase domain have been

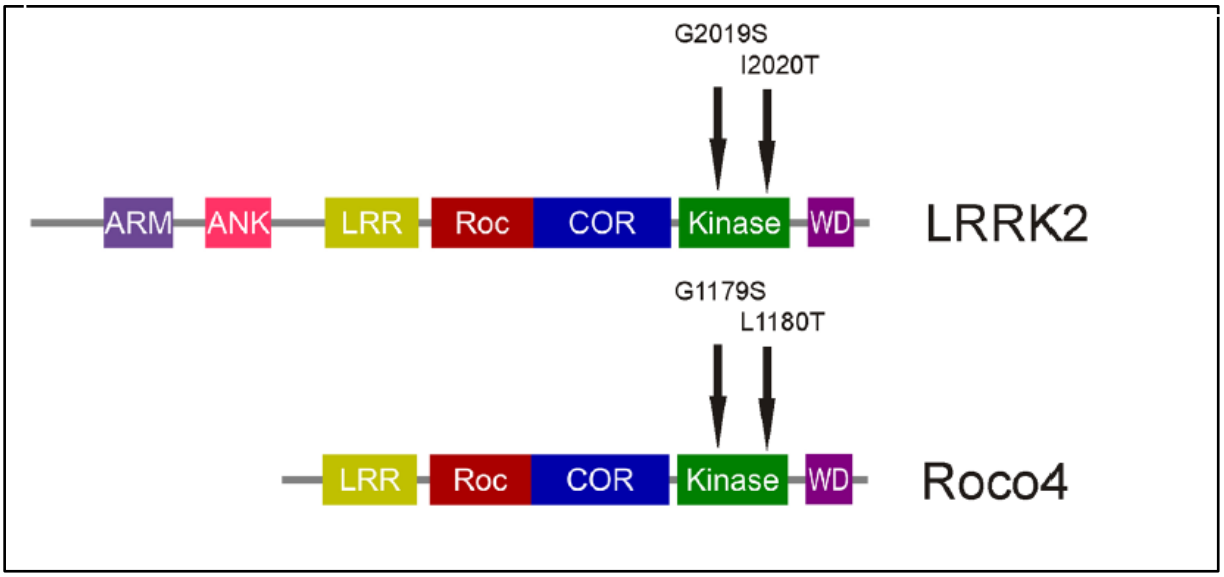

Figure 1: Domain topology of LRRK2 and Roco4 (Gilsbach BK, et al. 2014), showing two common mutations in the kinase domain.

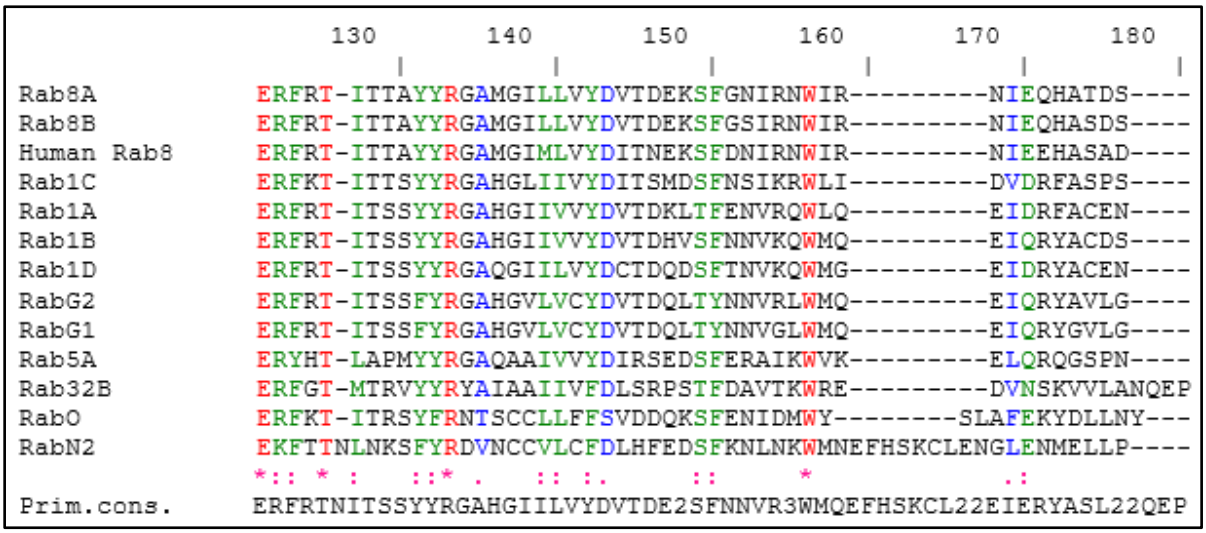

Figure 2: Sequence alignment of D. discoideum *Rabs and the human Rab. The conserved phosphorylation site is Threonine, marked with a red T.*

conserved in Roco4, and correspond to G1179S and I1180L, respectively (Fig. 1), and their behaviour is highly comparable to their LRRK2 counterparts. G1179S enhances kinase activity substantially, and I1180L decreases kinase activity slighty, if at all (Gilsbach BK, et al. 2014). Both mutations are able to phosphorylate LRRKtide, which is a known substrate of LRRK2, and the kinase domain of LRRK2 can substitute Roco4 kinase *in vivo* (Gilsbach BK, et al. 2012).

The main focus of this study is to determine whether various Rab proteins are substrates of Roco4 *in vitro,* and whether they exhibit any protein-protein interaction. Rabs are chosen on their conserved phosphorylation site in the Switch-2 region, which is similar to the phosphorylation sites of human Rabs that are known substrates of LRRK2 (Fig. 2). The Rab proteins and Roco4 kinase domain will be cloned in *E. coli* and purified using established protein purification methods. Radioisotope kinase assays will be used to measure kinase activity of the kinase domain of Roco4 on various Rab proteins, and radioisotope kinetics assays will determine protein kinetics. The protein-protein interactions will be characterized through protein pull-downs. We hope to identify the mechanism of kinase activity in Roco4, to hopefully improve the kinase inhibitors discussed earlier.

Furthermore, developmental studies of wildtype AX2 strains and *roco4-* strains will provide insight in the lifecycle of *D. discoideum* and intercellular activity of Roco4 proteins. To illustrate the pathways affected by Roco4 in presence of light (Gilsbach BK, et al. 2012), phototaxis experiments will be performed with wildtype *D. discoideum* and the *roco4*$^{-}$ strain.

Materials and methods

***D. discoideum* strains, developmental studies and phototaxis experiment.** Strains of *D. discoideum* used for this study were AX2 (wildtype) and *roco4*$^{-}$. They were germinated with *Klebsiella aerogenes* and grown in Petri dishes with 10 mL HL5 media at 21°C, or in shaking cultures with at least 25 mL HL5. To kill the remaining *K. aerogenes* 1:1000 Hygromycin or G418 (depending on antibiotic resistance marker in strain) was added. Cells were allowed to grow to a maximum density of 1 x 10^7 cells/mL.

To study the developmental cycle of *D. discoideum*, cells were deprived of nutrients and medium by washing with PB (pH 6.5) and put on non-nutrient agar plates. Pictures were taken under a light microscope for 48hrs or until fruiting bodies were formed. Magnification was set at 1.6x magnification, except for the pictures t = 6hrs, which were taken at 6.6x magnification.

For the phototaxis experiment, a v-shaped cut was made in NNA plates using a scalpel. AX2 and *roco4*$^{-}$ cells were added in the cut and plates were placed inside a plastic dark chamber with a slit cut out the front, so light only enters from one side. Cells were kept in constant light for 3 days, so both AX2 and *roco4*$^{-}$ can go through all developmental stages. Afterwards, a plastic sheet was places over each plate and this was stained with Coomassie to make the trails visible. Length of the slug trails were measured in ImageJ Fiji to quantify phototaxis.

PCR and quick change. PCR (extension time: 50s, annealing temperature:55°C) was performed. For the *rab* genes, the corresponding forward and reverse primers were selected and added to the PCR mix. For PCR cDNA (T=4,5) of *D. discoideum* was used, and it was performed both with and without DMSO. Quick change PCR (extension time: 7 min, annealing temperature: 45°C) was done to induce phosphorylation affecting point mutations into Rab1D. Rab1D in pGEX-4TEV was used as a template, and it was

performed both with and without DMSO. After quick change, 0.5µL of Dpn1 was added for 24h to break down the original gene without added mutations, which was heat inactivated at 80°C the next day.

Cloning of Rab proteins and the Roco4 kinase domain. Eleven Rab genes in pBluescript vector (Rab1A, Rab1C, Rab1D, Rab5A, Rab8A, Rab8B, Rab32B, RabG1, RabG2, RabN2, RabO) were provided by K. E. Rosenbusch and H. Pots, and had to be cloned into pGEX-4TEV or pPROEX HTb. Enzymatic digestion was done to cut the *rab* gene out of the pBlue vector, and products were loaded on a 1% agarose gel and purified using the gel purification kit. Gene inserts were ligated to other pGEX-4TEV or pPROEX HTb and used to transform DH5α *E. coli* cells. Colonies were then tested on whether they contained the insert in the right orientation, and these were then sent for sequencing.

Protein expression and protein purification. *E. coli* Rosetta cells were transformed with Rab in pGEX-4TEV/pPROEX HTb on a Petri dish, and then inoculated in a 120mL LB culture overnight with 1:1000 Ampicillin and 1:1500 Chloramphenicol. 25mL of this culture was added to a 2.5L flask with 100 µg/mL Ampicillin and 36µg/mL Chloramphenicol, using a total of 4 flasks. They were kept at 37°C on a shaker to multiply until the OD_{600} reached 0.6 – 0.8. To induce protein expression, 0.1 nM/mL IPTG was added to the flasks. Cells were then spun down and resuspended in standard buffer (150 mM NaCl, 30mM Tris--HCl, 5 mM $MgCl_2$, 3 mM DTT/DTE, 5% glycerol) and sonified/lysed. Proteins were purified by loading them on either a GSH-column or a His-column, subsequently followed by a size-exclusion column. GSH column was washed with standard buffer and washing buffer (350mM KCl in standard buffer), and elution buffer (20mM Gluthathion in standard buffer, pH 7.5) was used to elude the protein. Protein was concentrated to a volume of 250 – 500 µL and concentration was measured.

***D. discoideum* transformation.** To transform *D. discoideum* 2 to 4 x 10^7 cells were taken. 375 µL electrolysis buffer (250mM sucrose, 10mM PB) was added. 5 µL plasmid was pipetted on the wall of an electrolysis cuvette and the cells were added. Cuvette was kept 5 minutes on ice and then electroshocked at 500V, 500V/C, 50µF and 13Ω. 4 µL 0.1M MgCl2/CaCl2 was added to a new Petri dish and the cells were spread and allowed to attach to the surface before 10mL HL5 media was added. Then the appropriate antibiotics were added, either immediately (G418, neomycin) or after 24hrs (hygromycin). Cells were allowed to grow and recover for a week before any further experiments were performed.

Radioisotope kinase assay and radioisotope kinetics assay. Kinase activity of the Roco4 kinase domain on various Rabs was determined with radioisotope kinase assays. 100 µM substrate was added to a kinase buffer (25 mM Tris, 15 mM MgCl2, 20mM β-glycerol phosphate, 1 mM NaF, 1mM EGTA, 1mM Na3VO4, and 2mM DTT). Hot (radioactive) and cold ATP were added together before the start of the experiment. Reaction was started by adding radioactive ATP^{32} to the reaction mix and 20µL of the reaction mix was pipetted onto a nitrocellulose membrane. Reaction was stopped using 100mM EDTA and membrane was washed with 50mM phosphoric acid. Membranes were allowed to dry before scintillation counting. Radioisotope kinetics assays were performed in the same way.

Protein pull-down assays. For a pulldown 1 x 10^8 *D. discoideum* cells with Roco4-GFP (*roco4-,* pDM363) or free GFP (AX2, pDM317) were required. Cells were lysed in 2.5mL *Dictyostelium* lysis buffer (50mM Tris, 50mM NaCl, 5mM DTT, 5mM $MgCl_2$, 1% protease inhibitor, 1% Triton X) and kept on ice for 30 minutes to lyse the cells. If this did not lyse the cells sufficiently, they would be sonified for 3 times 2 minutes. Beads were spun down and washed with standard buffer (see 'Protein expression and protein purification') and were added to the supernatant of spun down lysed cells. Both GSH- and magnetic beads were used at different experiments. Then either 20µL Rab protein or 20µL GST were added and the tube was put at 4°C on a rotator for 3 – 4 hours. Subsequently, the cells were washed with standard buffer, and 1:1 4 x loading buffer was added and boiled for 10 minutes. Samples were then loaded onto a 12% SDS-PAGE gel.

Results

***D. discoideum* developmental studies.** Phenotypes of AX2 and r*oco4*$^-$ *D. discoideum* cells on NNA plates are depicted in Fig. 3. These images clearly show the lifecycle of healthy AX2 cells; from the cell streams at 6 h, to mounds and the formation of slugs at 18 h, to slug migration at 22 h, and formation of the fruiting bodies at 24 h and later. As expected, *roco4*$^-$ cells clearly have a developmental defect, as they take much longer to grow; first slugs are seen after 16-20h, first spores appear at around 72h. Evidently, the fruiting bodies of *roco4*$^-$ cells are faulty, causing the spore heads to lay flat across the surface of the plate instead of in the air.

***D. discoideum* phototaxis experiment.** AX2 slugs (Fig. 4, right) clearly all stream towards the light (direction of light shown with red arrow). The *roco4*$^-$ slugs (Fig. 4, left), do not exhibit such behaviour. They seem to be going in random directions and not directly towards the light, like the wildtype slugs. Phototaxic behaviour is quantified by measuring the length of the slug trails in ImageJ Fiji (Fig. 5). Length is expressed in pixels and is relative.

Purified Rabs. Eleven Rab proteins were planned for purification and investigation in this study. The genetic sequences encoding for various Rab proteins cloned in a commercially available pBluescript vector were

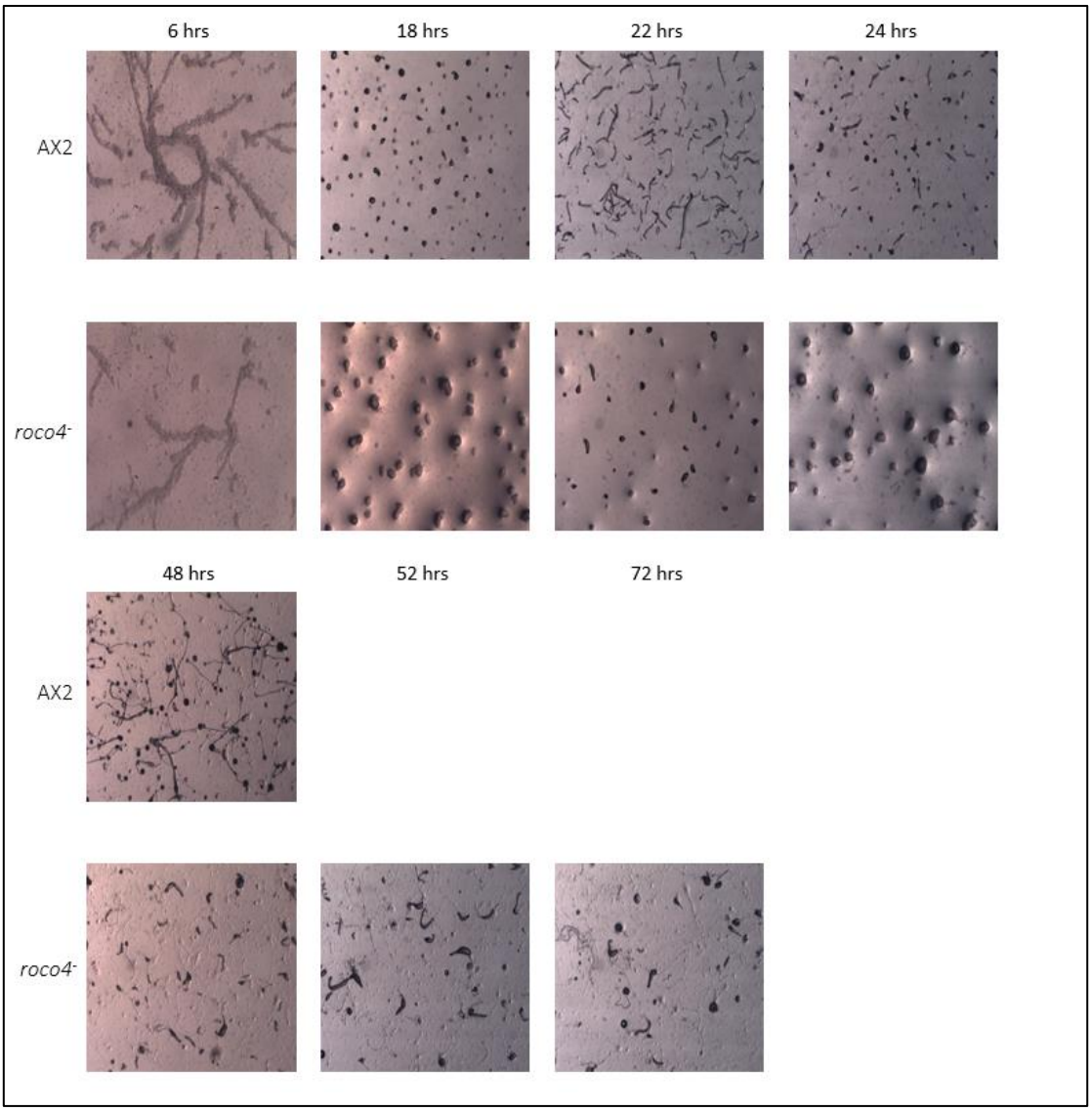

Figure 3: Pictures of phenotypes of AX2 and roco4- cells grown on NNA plates over time. Magnification at all time points except 6hrs: 1.6x. Magnification at t = 6hrs: 6.6x.

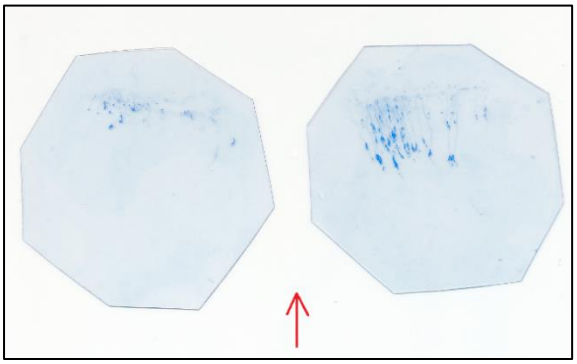

Figure 4: Phototaxis experiment. AX2 (right) show streaming towards the light (red arrow), whereas roco4- (left) cells show hardly any movement

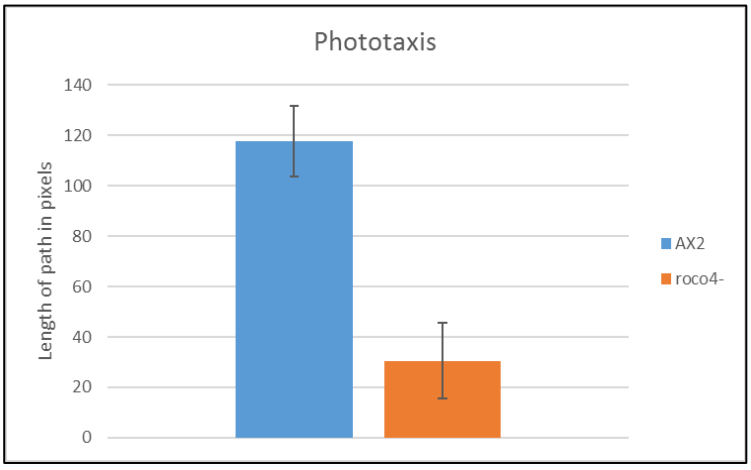

Figure 5: Quantified phototaxis. Length of the slug's path is measured in pixels. AX2 cells display significantly better phototactic behavior than roco4- cells (p = 0.05)

Name of Rab	Purified
1A	Yes
1C	Yes
1D	Yes
5A	Yes
8A	Yes
8B	Yes
32B	Yes
G1	Yes
G2	No*
N2	No*
O	Yes

Table 1: List of Rabs we intended to purify for this study, and whether or not we succeeded.

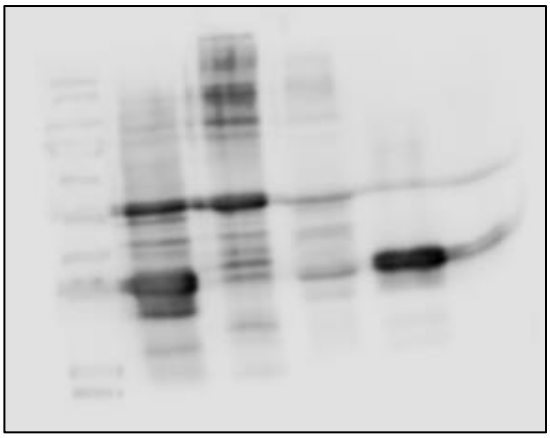

Figure 6: Western Blot of RabG2-GST samples at various stages of the purification process, Row 1: RabG2 protein purified via FPLC. Row 2: Cell lysate. 3. Cell pellet. Row 4. RabG2 injected.

given to us by H. Pots. He had already purified Rab1C, Rab1D, Rab5A, Rab8A, and RabG1.

Table 1 shows the eleven Rab proteins we intended to purify and whether or not purification was successful. We found that we were unable to clone RabN2 into either a pGEX-4TEV or a pProEX HTb vector; missense point mutations kept getting introduced for unknown reasons when cloning into these vectors, even though synthesis of the genetic sequence encoding for RabN2 via PCR was repeated. RabG2 was cloned in pGEX-4TEV without apparent issues, however, after purification the SDS-PAGE gel (12% resolving gel, 4% stacking gel) and Western blot it was evident that the majority of the purified protein represented GST (Fig. 6), instead of RabG2-GST. It is possible that this protein is misfolded or unstable when bound to a tag of this size.

The purified Rabs were used for radioisotope kinase assays, radioisotope kinetics assays, and protein pull-down assays.

Radioisotope kinase assays. A total of 11 radioisotope kinase assays were performed, with Roco4 kinase as blank, LRRKtide as positive control, and 9 different Rabs (Fig. 7). Data for Roco4 kinase as a blank were acquired from M. Tripathi. The scintillation counter counts two signals per membrane in different ways; projected as signal A and signal B. We chose to only display signal A, as the results are virtually the same, but this method of measuring is more reliable. The kinase assay of Rab1D was repeated once, to see whether the high amount of phosphorylation could be replicated. Rab8B and the first assay of RabO were not tested in duplicate, therefore no standard deviation could be calculated, and no t-tests could be done on the results of this Rab.

As expected, Roco4 kinase phosphorylates LRRKtide strongly. Interestingly, Rab1D exhibited remarkable phosphorylation by Roco4 kinase compared to the rest of the Rabs. Due to its promising phosphorylation, Rab1D was tested in a second radioisotope kinase assay, where it also showed a greatly increased signal. The first radioisotope assay with Rab1D is significant, as shown by unpaired T-test results ($p = 0.05$) in table 2. T-tests were performed on signal B. Although Rab8B also showed positive results, this assay was not performed in duplicate, making it impossible to determine whether the results are significant. Furthermore, results of phosphorylation of Rab32B and RabG1 are also significant. Future research into this topic will have to test phosphorylation of Rab8B further to determine whether Rab8B is a substrate for Roco4 kinase. Besides Rab1D, phosphorylation of Rab32B and RabG1 are also significantly increased compared to the Roco4 kinase blank. However, because these Rabs don't show such a remarkable increase in signal as seen with Rab1D, we've decided to focus on Rab1D for further experiments.

Radioisotope kinetics assays. Because Rab1D showed such high amounts of phosphorylation during radioisotope kinase assays, kinetics assays were performed. A total of 4 kinetics assays of Rab1D were done. As with the radioisotope kinase assays, the scintillation counter counts two signals per membrane in different ways. For the graph, signal A was used (Fig. 8). Significance of results of the kinetics assays are determined with unpaired T-tests on channel B.

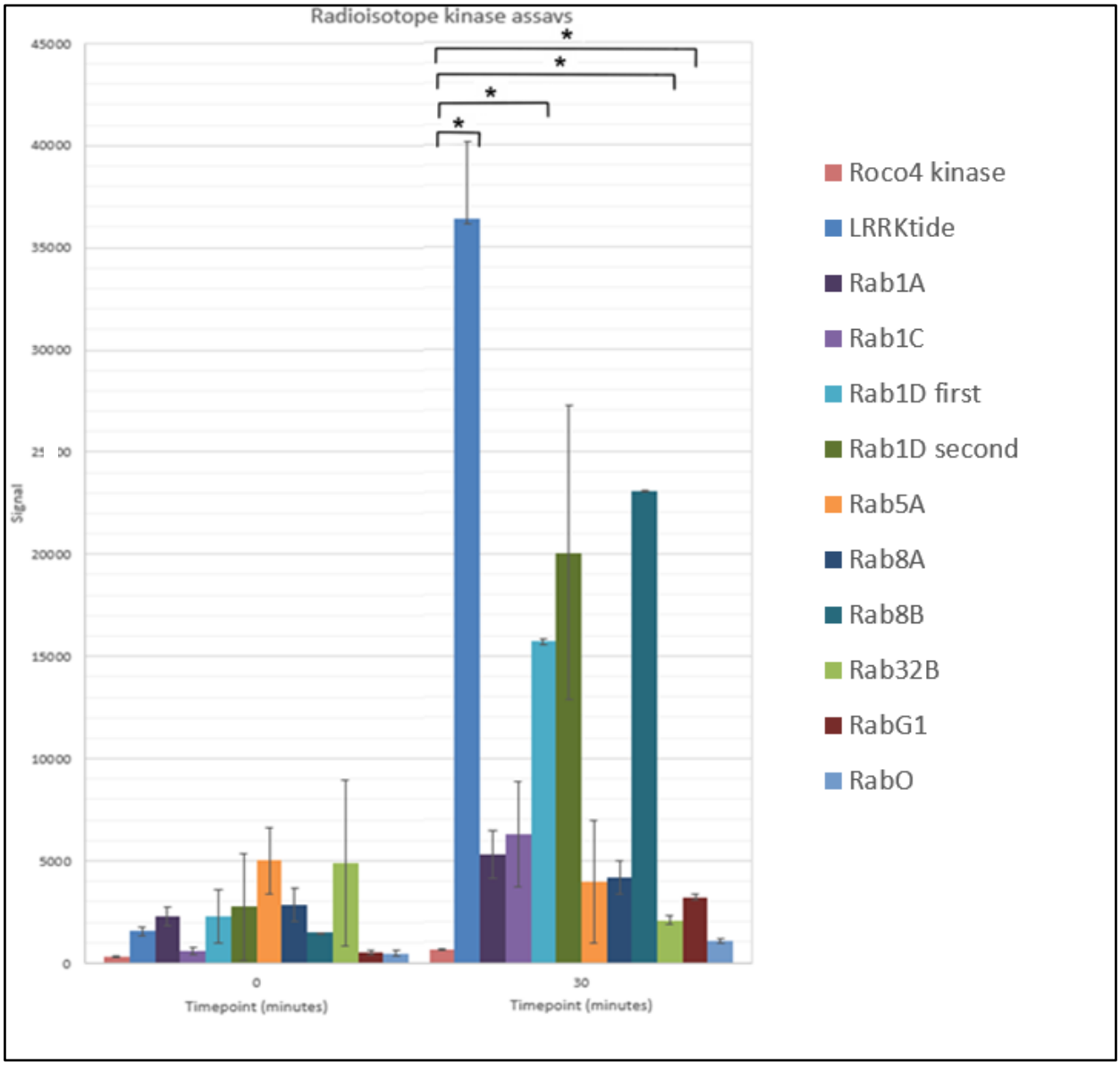

Figure 7: Radioactive kinase assays graphs, showing the signals of the individual Rabs when measured for radioactivity at t=0 and t=30 minutes. LRRKtide is highly phosphorylated, as this is a known substrate of Roco4 kinase. Rab1D and Rab8B both stand out, showing a lot of phosphorylations. Asterisks mark significance compared to the Roco4 kinase blank (p = 0.05).

	LRRKtide	Rab1A	Rab1C	Rab1D first	Rab1D second	Rab5A	Rab8A	Rab32B	RabG1	RabO
Roco4 kinase 0	2.57881E-05	0.099274526	0.259173442	0.27922695	0.421451118	0.154400658	0.145145285	0.040484347	0.26161237	0.584794497
Roco4 kinase 30	2.7136E-06	0.109873709	0.19823399	0.003013827	0.163026894	0.35919888	0.104077951	2.97766E-06	0.02315945	0.059312467

Table 2: T-test results of the kinase assays. Significant results are shown in green (p = 0.05)

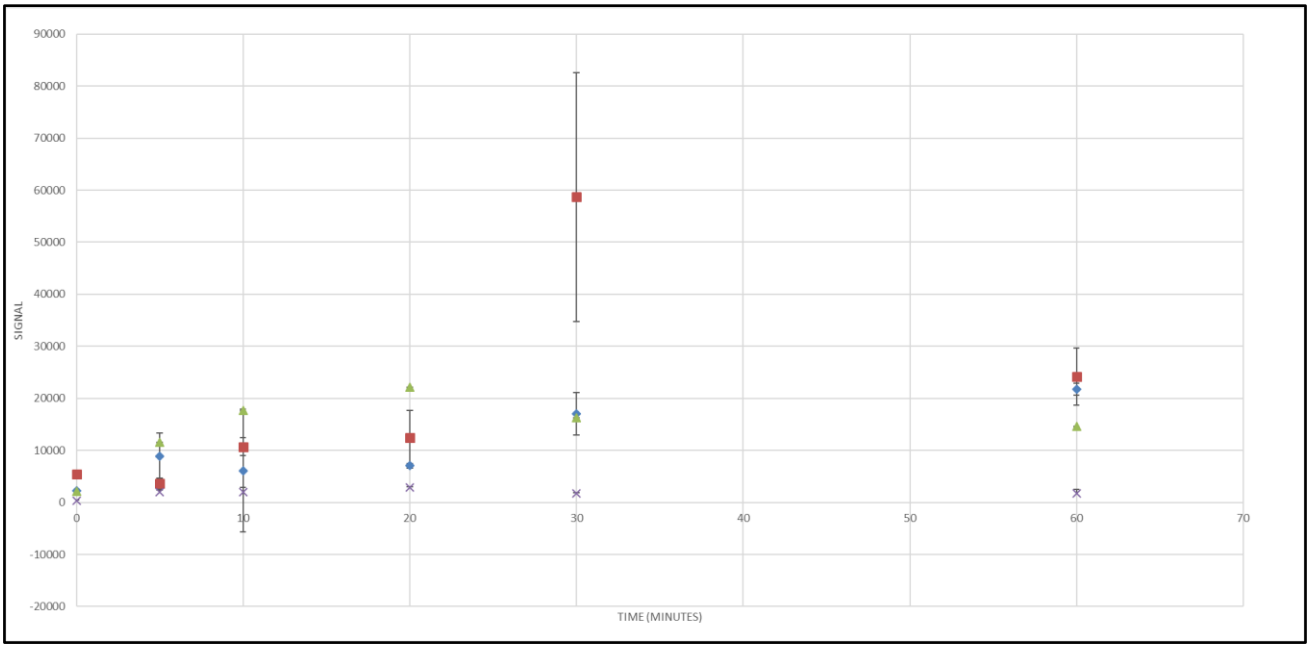

Figure 8: Radioisotope kinetics assay of Rab1D. Four kinetics assays were performed and are shown in different colors and symbols. In the assay displayed as purple crosses a tenfold less o f ATP was used, therefore results are not comparable to the other assays.

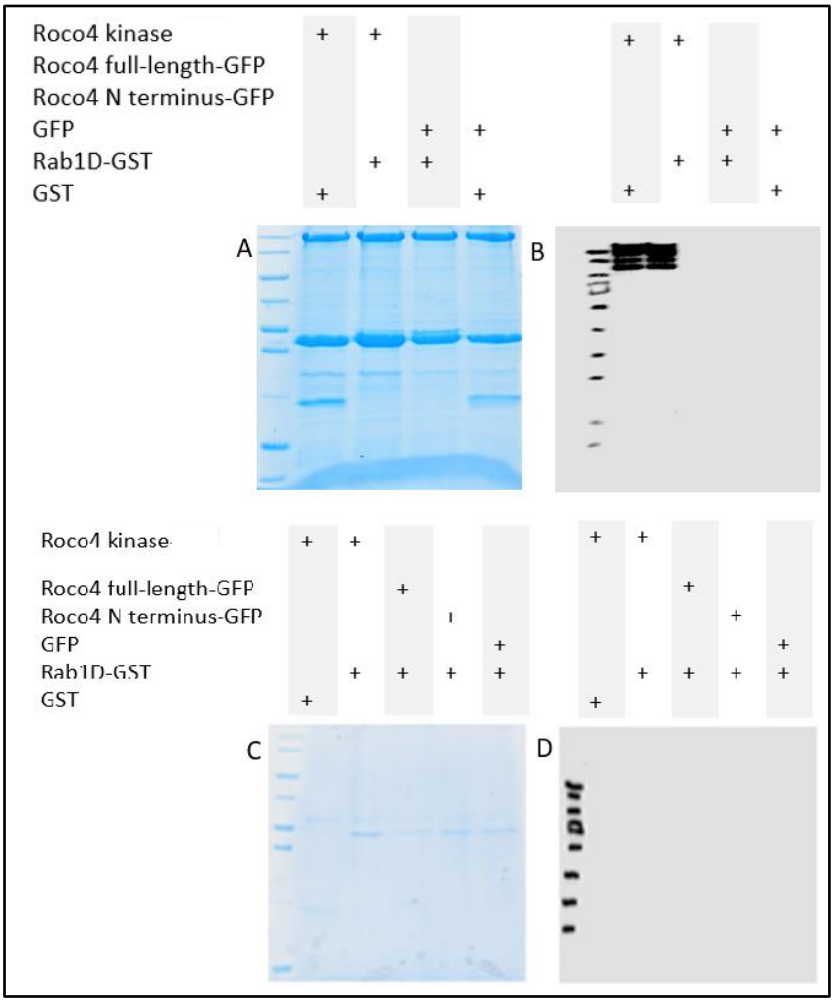

Figure 9: SDS-PAGE gels and Western Blots of the pull-down assays. Images on the same row depict the same assay. A and B are from a GSH bead pull-down assay, C and D from a magnetic bead pull-down.

It is clear that signal first strongly increases over time, but gradually reaches a plateau after about 30 minutes. As time passes by, more substrate will have reached a kinase to react with, until there is no more unphosphorylated Rab1D left in the reaction mix to phosphorylate. Therefore, signal will not increase after a certain amount of time has passed by. This means that Rab1D is certainly a substrate for Roco4 kinase. The kinetics assay displayed as purple crosses was done with tenfold less ATP and did not follow a Michaelis-Menten curve, possibly due to an unavailability of ATP for all present Roco4 kinase proteins to phosphorylate Rab1D.

Protein pull-down assays. Rab1D proved to be such a promising substrate for Roco4 kinase that pull-down assays were performed to determine whether Rab1D physically interacts with Roco4 kinase, full-length Roco4, or the N-terminus of Roco4. Five pull-down assays were done; three times with GSH beads which bind to GST proteins, and twice with magnetic beads to which any antibody would bind. Negative controls were added to each assay.

Reaction mixes with GSH beads:

- Roco4 kinase + Rab1D-GST
- Roco4 kinase + GST
- Roco4 N-terminus-GFP + Rab1D-GST
- Roco4 N-terminus-GFP + GST
- GFP + Rab1D-GST
- GFP + GST

Reaction mixes with magnetic beads:

- Roco4 kinase + GST
- Roco4 kinase + Rab1D-GST
- Roco4 N-terminus-GFP + Rab1D-GST
- Roco4 full-length-GFP + Rab1D
- GFP + Rab1D-GST

Fig. 9 shows the SDS-PAGE gels and Western blots of two pull-down assays; the first being a pull-down with GSH beads and the second with magnetic beads. Unfortunately, there are no clear results, as there are contamination bands found in every SDS-PAGE gel and Western blot. In the SDS-PAGE gel you would not expect to see any bands, as the amount of inserted protein should in this experiment in theory be lower than the detection minimum (10 mg protein).

We can confirm Rab1D does not directly interact with Roco4 kinase, full-length or the N-terminus in any way, as none of the five pulldowns showed clear indications of Roco4 being present in the any of the samples.

Discussion

In this article we aimed to show the effect on the *D. discoideum* phenotype after knocking out *roco4*, whether any of the tested Rab proteins are a substrate of the *D. discoideum* Roco4 protein, and we hoped to shed some light on the mechanisms of kinase activity in Roco4.

During the development studies the wildtype AX2 cells successfully aggregate, stream, form a mound, migrate as slugs, and eventually become fruiting bodies after 24 hours. Development of *roco4*$^-$ cells is evidently impaired; these cells develop slower than their wildtype counterparts, suggesting Roco4 is involved in regulating the developmental cycle of *D. discoideum*. Furthermore, the fruiting bodies of *roco4*$^-$ cells are flawed; they lay flat across the surface of the petri dish rather than standing upright. This fragile phenotype is caused by missing cellulose due to lack of a functional Roco4, as reported by van Egmond WN, et al. 2010.

As expected, the AX2 slugs in the phototaxis experiment exhibited perfect streaming behaviour towards the light source. The *roco4*$^-$ slugs did not migrate towards the light; the slugs hardly migrated, nor showed any other signs of light sensitivity or light detection. After quantification it is clear that these differences in phototaxis are significant. The fact that *roco4*$^-$ cells show such a strikingly different phenotype compared to AX2 cells implies a role for Roco4 in phototactic signalling pathways.

Francoine LM, et al. have reported in 2010 that impairment of phototaxis is a hallmark of mitochondrial dysfunction in *D. discoideum*. This study tested different forms of mitochondrial disease in *D. discoideum* and found that phototactic signalling pathways were always impaired. While these pathways are not fully elucidated, it is assumed some proteins involved in the process of phototaxis are also involved in energy stress signalling. Development is another phenotype affected by mitochondrial dysfunction, something we also saw in the *roco4*$^-$ cells in our development studies. Human LRRK2 of the same Roco family of proteins is also known to be involved in mitochondrial dysfunction (Esteves AR, 2016) (Winner B, et al. 2011). This implies that Roco4 might play a role in the (downstream) signalling pathways of the mitochondria.

We intended to test whether eleven Rabs are substrates of Roco4. These Rabs were chosen by their conserved phosphorylation site compared to LRRK2 substrate Rabs, which indicates a higher chance of being phosphorylated by Roco4. Out of eleven Rabs, we were able to purify nine and test these with radioisotope kinase assays, Rab1D and Rab8B showed significantly increased signals at 30 minutes compared to the blank with just Roco4 kinase (table 2). They are phosphorylated by the kinase domain of Roco4. Their signal was also substantially higher than the signal of any other Rab at time point 30 minutes. Unfortunately, Rab8B was not tested in duplicate. It could therefore be possible the increased signal was merely happenstance. The radioisotope kinase assay will have to be repeated in order to exclude this possibility and prove that Rab8B is also a substrate of Roco4 kinase, and therefore possibly of LRRK2. Rab32B and RabG1 also showed significantly increased phosphorylation compared to the Roco4 kinase blank, but because these signals were not as high, we decided to pursue Rab1D. The second kinase assay done with Rab1D did not turn out to have significantly enhanced phosphorylation. This is most due to the large standard deviation in the signal data of this assay.

To be sure whether Rab1D truly is a substrate of Roco4, Rab1D was further investigated using radioisotope kinetics assays. The graphs displayed Michaelis-Menten-like curves; signal kept increasing until it reached a plateau after about 30 minutes. This means that Rab1D is indeed a substrate for Roco4 kinase, as over time all available Rab1D was phosphorylated by Roco4 kinase, and the radioactive signal from incorporated ATP in phosphorylated Rab1D can increase no more. As Roco4 is homologous to human LRRK2 and other human Rabs have already been known to be substrates of LRRK2 (Steger M et al. 2016) (Yun HJ et al. 2015).

Regrettably, the pull-down assays performed on Rab1D show mainly contamination and no clear indication Rab1D binds to Roco4. Therefore, it is unlikely that Rab1D interacts (strongly) with Roco4 full-length or with either the kinase domain or N-terminus. Their interaction is limited to phosphorylation by the kinase domain and no binding occurs between Rab1D and the N terminus of Roco4, or any other domain of Roco4. After phosphorylation, the proteins may immediately dissociate.

Rab1D is a GTPase which acts as a molecular switch. Its predicted functions (according to Dictybase.org, as there is not data about Rab1D knock-outs yet,) are ER-to-Golgi-mediated transport, small GTPase-mediated signal transduction and micropinocytosis. Steger M, et al. reported some Rabs they examined did indeed get overphosphorylated due to LRRK2 dysfunction. The functioning of Rabs might be compromised in PD patients due to the increase in phosphorylation by malfunctioning LRRK2, perhaps contributing to the disease's phenotype. It could be possible that this also holds true for Roco4. Unfortunately, this would not directly explain the *roco4*$^{-}$ phenotype we saw, as the observed defects were limited to development rate and phototaxis. It is possible that Rab1D is a part of intercellular pathways that regulate development and phototaxis, however our findings cannot confirm this.

With the knowledge that Rab1D and Rab8 are (potential) substrates for the Roco4 kinase domain, we can investigate these Rabs further, as well as their link to Roco4 (and LRRK2). Future experiments may include determining the kinetics of Rab8B, and studying the kinetics of both Rab1D and Rab8B with full-length Roco4 and Roco4 G1179S, the conserved mutation of the most common PD associated point mutation G2019S in LRRK2, rather than solely the Roco4 kinase domain. To ensure Rab1D is being phosphorylated at the site we suspect, the radioactive kinase assay can be repeated, but instead of conventional Rab1D we can use Rab1D with specific point mutations. Rab1D T220A is not able to get phosphorylated, whereas Rab1D T220D is a phosphomimetic and should be constitutively active. This can also be tested *in vivo*. In order to study the effect of Rab1D *in vivo*, it can be introduced into both the wild type and the *roco4*$^{-}$ strains of *D. discoideum* and *roco4G1179S* cells. It would be interesting to learn what would happen when the kinase of Roco4 is overactive due to this mutation (which is comparable to some forms of PD), what effect Roco4G1179S would have on the phosphorylation of Rab1D and the corresponding downstream pathways, and whether the use of kinase inhibitors affects these pathways.

Concluding, this study shows that the phenotype of *D. discoideum* drastically changes when *roco4* is knocked out; the slugs no longer possess the ability to migrate towards light using phototaxis, the rate of development is significantly impaired, and due to the loss of cellulose the stalks are weak, causing the spore heads to lay on the surface of the plates. These phenotypes are linked to mitochondrial dysfunction, indicating Roco4 is involved in signalling pathways in the mitochondria. Rab1D and Rab8B proved to be substrates for Roco4. These results could suggest that

in PD, where the kinase domain of LRRK2 is overactive, the phosphorylation of Rab proteins may be increased, which may contribute to the phenotype belonging to PD.

References

Berwick DC, Harvey K (2012) LRRK2 functions as a Wnt signaling scaffold, bridging cytosolic proteins and membrane-localized LRP6. Hum.Mol.Genet. 21, 4966 – 4979.

Cookson MR (2010) The role of leucine-rich repeat kinase 2 (LRRK2) in Parkinson's disease. Nat. Rev. Neurosci. 11(12), 791 – 797.

Cooper AA, et al. (2006) α-Synuclein blocks ER-Golgi traffic and Rab1 rescues neuron loss in Parkinson's models. Science 313(5785), 324 – 328.

Covy JP, Giasson BI. (2009) Identification of compounds that inhibit the kinase activity of leucine-rich repeat kinase 2. Biochem. Biophys. Res. Commun. 378(3), 473 – 477.

Dächsel JC, et al. (2010) A comparative study of LRRK2 function in primary neuronal cultures. Parkinsonism Relat. Disord. 16, 650–655.

Deng X. (2011) Characterization of a selective inhibitor of the Parkinson's disease kinase LRRK2. Nature Chemical Biology. 7, 203–205.

Egmond WN van, et al. (2010) Characterization of the Roco protein family in Dicty. Eukaryotic Cell. 751 – 761.

Esteves AR, Cardoso SM (2016) LRRK2 at the crossroad between autophagy and microtubule trafficking: insights into Parkinson's Disease. Neuroscientist. Epub ahead of print.

Fell MJ, et al. (2015) MLi-2, a potent, selective, and centrally active compound for exploring the therapeutic potential and safety of LRRK2 kinase inhibition. J Pharmacol Exp Ther. 355(3), 397-409.

Francoine LM, et al. (2010) The *Dictyostelium* model for mitochondrial disease. Seminars in Cell & Developmental Biology. 22, 120-130.

Gilsbach BK, et al. (2012) Roco kinase structures give insights into the mechanism of Parkinson disease-related leucine-rich-repeatkinase 2 mutations. Proceedings of the National Academy of Sciences of the United States of America. 109, 10322 – 10327.

Gilsbach BK, Kortholt A. (2014) Structural biology of the LRRK2 GTPase and kinase domains: implications for regulation. Frontiers in Molecular Neuroscience. 7(32).

Gitler AD, et al. (2008) The Parkinson's disease protein α-Synuclein disrupts cellular Rab homeostasis. Proceedings of the National Academy of Sciences of the United States of America. 105(1), 145 – 150.

Gómez-Suaga P, et al. (2014) LRRK2 delays degradative receptor trafficking by impeding late endosomal budding through decreasing Rab7 activity. Human Molecular Genetics. 23, 6779 – 6796.

Healy DG, et al. (2008) Phenotype, genotype, and worldwide genetic penetrance of LRRK2-associated Parkinson's disease: a case-control study. Lancet Neurol. 7(7), 583 – 590.

Herzig MC, et al. (2011) LRRK2 protein levels are determined by kinase function and are crucial for kidney and lung homeostasis in mice. Hum.Mol.Genet. 20, 4209 – 4223.

Ho, FY, et al. (2014) The potential of targeting LRRK2 in Parkinson's Disease. InTech. Available from: http://www.intechopen.com/books/a-synopsis-of-parkinson-s-disease/the-potential-of-targeting-lrrk2-in-parkinson-s-disease

Jaleel M, et al. (2007) LRRK2 phosphorylates moesin at threonine-588: characterization of how Parkinson's disease mutants affect kinase activity. Biochem J. 405(2), 307 – 317.

Khan NL, et al. (2005) Mutations in the gene LRRK2 encoding dardarin (PARK8) cause familial Parkinson's disease: Clinical, pathological, olfactory and functional imaging and genetic data. Brain. 128, 2786–2796.

Lees AJ, et al. (2009). Parkinson's Disease. Lancet. 373, 2055 – 2066.

Maree AFM, et al. (1999) Phototaxis during the slug stage of Dictyostelium discoideum: a model study. Proceedings of the Royal Society B: Biological Sciences. 266(1426), 1351.

Marin I, et al. (2008). The Roco protein family; a functional perspective. Phaseb. J. 22(9), 3103 – 3110.

Nails MA, et al. (2011) Imputation of sequence variants for identification of genetic risks for Parkinson's disease; a meta-analysis of genome-wide association. Lancet. 377(9766), 641 – 649.

Sanchez SJ, et al. (2009) Genome-wide association study reveals genetic risk underlying Parkinson's disease. Nat. Genet. 41(12), 1308 – 1312.

Steger M, et al. (2016) Phosphoproteomics reveals that Parkinson's disease kinase LRRK2 regulates a subset of Rab GTPases. eLife. 5:e12813.

Su Y, Qi X. (2013) Inhibition of excessive mitochondrial fission reduced aberrant autophagy and neuronal damage caused by LRRK2 G2019S mutation. Human Molecular Genetics. 22(22), 4545–4561.

Su Y, Qi X. (2013) Inhibition of excessive mitochondrial fission reduced aberrant autophagy and neuronal damage caused by LRRK2 G2019S mutation. Human Molecular Genetics. 22(22), 4545 – 4561.

West AB, et al. (2005) Parkinson's Disease-associated mutations in leucine-rich repeat kinase 2 augment kinase activity. Proc. Natl. Acad. Sci. U.S.A. 15, 16842 – 16847.

Winner B, et al. (2011) Adult neurogenesis and neurite outgrowth are impaired in LRRK2 G2019S mice. Neurobiol. Dis. 41, 706–716.

Yun HJ, et al. (2015). An early endosome regulator, Rab5B, is an LRRK2 kinase substrate. J. Biochem. 157(6), 485 – 495.